J|A|C|S
ARTICLES
Published on Web 04/01/2006

Oxidative Addition of Dihydrogen to (η^6-Arene)Mo(PMe_3)$_3$ Complexes: Origin of the Naphthalene and Anthracene Effects

Guang Zhu, Kevin E. Janak, Joshua S. Figueroa, and Gerard Parkin*

Contribution from the Department of Chemistry, Columbia University, New York, New York 10027

Received November 29, 2005; E-mail: parkin@columbia.edu

Abstract: In contrast to the benzene and naphthalene compounds (η^6-PhH)Mo(PMe_3)$_3$ and (η^6-NpH)Mo(PMe_3)$_3$, the anthracene complex (η^6-AnH)Mo(PMe_3)$_3$ reacts with H_2 to undergo a haptotropic shift and give the η^4-anthracene compound (η^4-AnH)Mo(PMe_3)$_3H_2$. Density functional theory calculations indicate that the increased facility of naphthalene and anthracene to adopt η^4-coordination modes compared to that of benzene is a consequence of the fact that the Mo−(η^4-ArH) bonding interaction increases in the sequence benzene < naphthalene < anthracene, while the Mo−(η^6-ArH) bonding interaction follows the sequence benzene > naphthalene ≈ anthracene.

Introduction

It has long been known that indenyl complexes of the transition metals typically exhibit much more facile associative reactions than their cyclopentadienyl counterparts.[1,2] Indeed, the magnitude of the rate enhancement is so substantial that a special term was coined by Basolo to describe it, viz. the "indenyl effect".[3] The origin of the indenyl effect is associated with the fact that the indenyl ligand shows a greater tendency to adopt an η^3-coordination mode than does the cyclopentadienyl ligand, and the coordinative unsaturation that is provided by the ring slippage facilitates an associative mechanism. Not only are such haptotropic shifts now widely recognized to play a prevalent role in the chemistry of cyclopentadienyl, indenyl, and fluorenyl complexes,[4] but more facile ring slippage has also been proposed to account for the increased lability of naphthalene compared to that of benzene in metal−arene complexes, and this phenomenon has been referred to as the "naphthalene effect".[5,6] However, despite the many observations that naphthalene is more readily displaced than benzene, there are no experimental studies that quantify the influence of ring fusion on a well-defined reversible η^6/η^4 haptotropic shift.[7] Furthermore, the majority of studies pertaining to the influence of ring fusion have been concerned with complete arene displacement by donor ligands such as CO and PR_3, and we are aware of none involving oxidative addition of H_2, a reaction that is of considerable significance with respect to arene hydrogenation.[8] In this paper, we (i) provide evidence that ring fusion to an arene promotes the oxidative addition of H_2 to a metal center via facilitating an η^6-to-η^4 haptotropic shift and (ii) provide an explanation for the effect.

Scheme 1

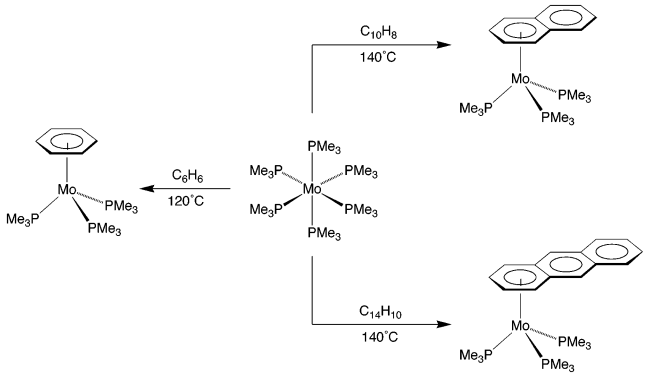

Results and Discussion

1. Synthesis of (η^6-ArH)Mo(PMe_3)$_3$ and Reactivity towards H_2. The η^6-arene compounds (η^6-PhH)Mo(PMe_3)$_3$,[9] (η^6-NpH)Mo(PMe_3)$_3$,[10] and (η^6-AnH)Mo(PMe_3)$_3$ may be conveniently obtained via reaction of Mo(PMe_3)$_6$ with the appropriate arene, namely PhH (benzene), NpH (naphthalene), and AnH (anthracene), as illustrated in Scheme 1. The molecular structures of (η^6-NpH)Mo(PMe_3)$_3$ and (η^6-AnH)Mo(PMe_3)$_3$ have been determined by X-ray diffraction, as illustrated in Figures 1 and 2. Examination of the Mo−C bond length data (Table 1)

(1) For early examples, see: (a) Hart-Davis, A. J.; Mawby, R. J. *J. Chem. Soc. (A)* **1969**, 2403−2407. (b) Hart-Davis, A. J.; White, C.; Mawby, R. J. *Inorg. Chim. Acta* **1970**, *4*, 441−446. (c) Jones, D. J.; Mawby, R. J. *Inorg. Chim. Acta* **1972**, *6*, 157−160.

(2) (a) Basolo, F. *Polyhedron* **1990**, *9*, 1503−1535. (b) Basolo, F. *Inorg. Chim. Acta* **1985**, *100*, 33−39. (c) Basolo, F. *New J. Chem.* **1994**, *18*, 19−24.

(3) (a) Rerek, M. E.; Ji, L. N.; Basolo, F. *J. Chem. Soc., Chem. Commun.* **1983**, 1208−1209. (b) Rerek, M. E.; Basolo, F. *J. Am. Chem. Soc.* **1984**, *106*, 5908−5912.

(4) (a) O'Connor, J. M.; Casey, C. P. *Chem. Rev.* **1987**, *87*, 307−318. (b) Alt, H. G.; Samuel, E. *Chem. Soc. Rev.* **1998**, *27*, 323−329. (c) Calhorda, M. J.; Veiros, L. F. *Coord. Chem. Rev.* **1999**, *185*−*186*, 37−51.

(5) (a) Thi, N. P. D.; Spichiger, S.; Paglia, P.; Bernardinelli, G.; Kündig, E. P.; Timms, P. L. *Helv. Chim. Acta* **1992**, *75*, 2593−2607. (b) Kündig, E. P.; Perret, C.; Spichiger, P. S.; Bernardinelli, G. *J. Organomet. Chem.* **1985**, *286*, 183−200.

(6) The ability to access an η^4-coordination mode is also of importance with respect to the product release step of the transition-metal-promoted functionalization of arenes. See, for example: (a) Semmelhack, M. F.; Chlenov, A.; Ho, D. M. *J. Am. Chem. Soc.* **2005**, *127*, 7759−7773. (b) Butler, I. S.; Uhm, H. L. *Comments Inorg. Chem.* **1988**, *7*, 1−16.

(7) For examples of η^6-to-η^4 haptotropic shifts of arene ligands, see: (a) Bennett, M. A.; Lu, Z.; Wang, X.; Bown, M.; Hockless, D. C. R. *J. Am. Chem. Soc.* **1998**, *120*, 10409−10415. (b) Boncella, J. M.; Green, M. L. H. *J. Organomet. Chem.* **1987**, *325*, 217−231.

10.1021/ja058107f CCC: $33.50

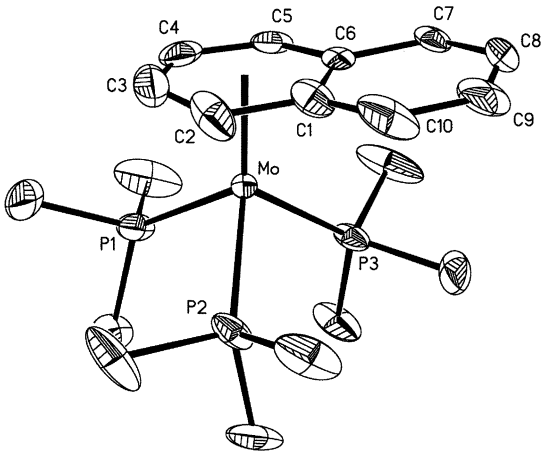

Figure 1. Molecular structure of (η^6-NpH)Mo(PMe_3)$_3$.

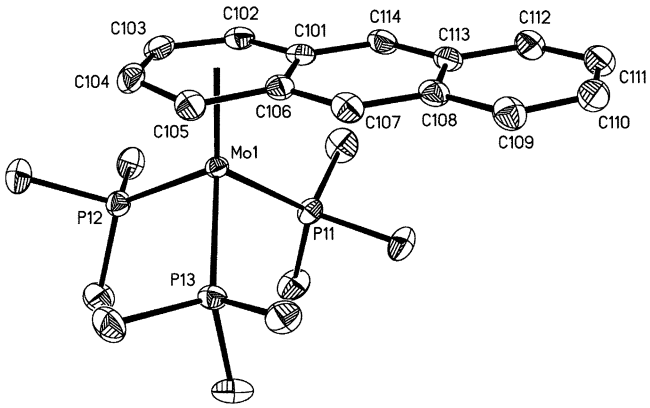

Figure 2. Molecular structure of (η^6-AnH)Mo(PMe_3)$_3$ (only one of the two independent molecules is shown).

Table 1. Selected Bond Lengths (Å) for (η^6-NpH)Mo(PMe_3)$_3$ and (η^6-AnH)Mo(PMe_3)$_3$

	(η^6-NpH)Mo(PMe_3)$_3$[a]	(η^6-AnH)Mo(PMe_3)$_3$[b,c]	
Mo(X)−C(Y2)	2.263(12)	2.297(3)	2.307(3)
Mo(X)−C(Y3)	2.245(16)	2.261(3)	2.270(3)
Mo(X)−C(Y4)	2.220(12)	2.285(3)	2.285(3)
Mo(X)−C(Y5)	2.270(10)	2.268(3)	2.267(3)
Mo(X)−C(Y1)	2.378(11)	2.405(3)	2.422(3)
Mo(X)−C(Y6)	2.404(8)	2.424(3)	2.419(3)
Mo(X)−P(Y′1)	2.381(3)	2.4274(8)	2.4342(8)
Mo(X)−P(Y′2)	2.418(3)	2.3930(9)	2.4354(8)
Mo(X)−P(Y′3)	2.393(3)	2.4350(7)	2.3976(9)

[a] X = Y = Y′ = no value. [b] X = 1, Y = 10, Y′ = 1. [c] X = 2, Y = 20, Y′ = 2.

indicates that the arene ligands are displaced from symmetric η^6-coordination towards a "flat" η^4-coordination mode.[11] Similar "flat-slipped" coordination modes have been observed for (η^6-AnH)Cr(CO)$_3$[12] and other (η^6-ArH)Cr(CO)$_3$ complexes which feature fused polycyclic arenes.[13,14] Another example of a "flat-slipped" η^6-arene compound is provided by Ti(η^6-AnH)(η^4-AnH)(dmpe), which contains both η^6- and η^4-coordinated anthracene ligands.[15,16] The origin of the displacement of the arene ligands in (η^6-NpH)Mo(PMe_3)$_3$ and (η^6-AnH)Mo(PMe_3)$_3$ has been addressed by using computational methods and is described in section 2.

Scheme 2

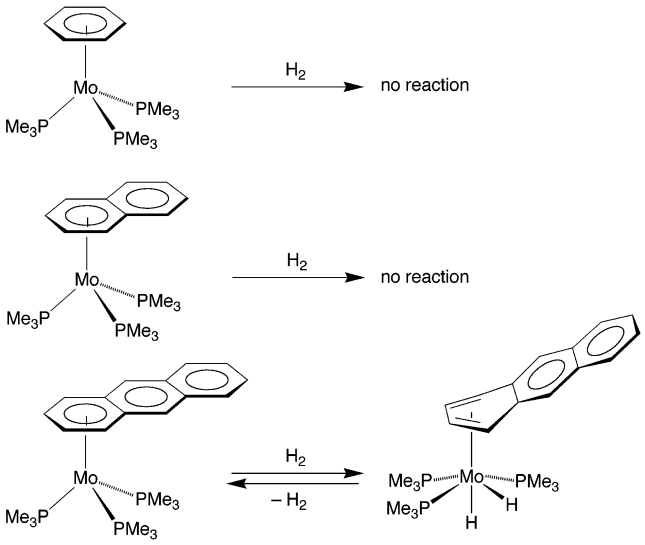

In view of the fact that the zerovalent (η^6-ArH)Mo(PMe_3)$_3$ derivatives are electron-rich (i.e., have high-energy occupied metal-based orbitals),[17] we considered that each would be susceptible towards oxidative addition of dihydrogen, cf. the facile formation of Mo(PMe_3)$_4H_4$ from Mo(PMe_3)$_6$.[18] However, in contrast to Mo(PMe_3)$_6$, (η^6-PhH)Mo(PMe_3)$_3$ is unreactive towards H_2 (1 atm) in benzene solution at 80 °C (Scheme 2).[19]

(8) (a) Widegren, J. A.; Finke, R. G. *J. Mol. Catal. A: Chemical* **2003**, *191*, 187−207. (b) Amer, I.; Amer, H.; Ascher, R.; Blum, J.; Sasson, Y.; Vollhardt, K. P. C. *J. Mol. Catal.* **1987**, *39*, 185−194.

(9) (η^6-PhH)Mo(PMe_3)$_3$ has been recently reported. See: (a) Ashby, M. T.; Asirvatham, V. S.; Kowalski, A. S.; Khan, M. A. *Organometallics* **1999**, *18*, 5004−5016. (b) Canestrari, M.; Green, M. L. H.; Izquierdo, A. *J. Chem. Soc., Dalton Trans.* **1984**, 2795−2801.

(10) (η^6-NpH)Mo(PMe_3)$_3$ has been previously reported. See ref 5a.

(11) For a review of the structures of metal−arene compounds, see: Hubig, S. M.; Lindeman, S. V.; Kochi, J. K. *Coord. Chem. Rev.* **2000**, *200*−*202*, 831−873.

(12) Hanic, F.; Mills, O. S. *J. Organomet. Chem.* **1968**, *11*, 151−158.

(13) Arrais, A.; Diana, E.; Gervasio, G.; Gobetto, R.; Marabello, D.; Stanghellini, P. L. *Eur. J. Inorg. Chem.* **2004**, 1505−1513.

(14) Müller, P.; Bernarddinelli, G.; Jacquier, Y. *Helv. Chim. Acta* **1992**, *75*, 1995−2008.

(15) The η^6-anthracene ligand is characterized by Ti−C bond lengths of 2.31−2.36 Å, while the Ti−C distances for the ring junction average 2.63 Å. See: Seaburg, J. K.; Fischer, P. J.; Young, V. G.; Ellis, J. E. *Angew. Chem., Int. Ed.* **1998**, *37*, 155−157.

(16) For other examples of η^4-anthracene complexes, see: (a) Brennessel, W. W.; Ellis, J. E.; Pomije, M. K.; Sussman, V. J.; Urnezius, E.; Young, V. G., Jr. *J. Am. Chem. Soc.* **2002**, *124*, 10258−10259. (b) Brennessel, W. W.; Ellis, J. E.; Roush, S. N.; Strandberg, B. R.; Woisetschläger, O. E.; Young, V. G., Jr. *Chem. Commun.* **2002**, 2356−2357. (c) Mashima, K.; Nakayama, Y.; Kaidzu, M.; Ikushima, N.; Nakamura, A. *J. Organomet. Chem.* **1998**, *557*, 3−12. (d) Müller, J.; Gaede, P. E.; Hirsch, C.; Qiao, K. *J. Organomet. Chem.* **1994**, *472*, 329−335. (e) Boese, R.; Stanger, A.; Stellberg, P.; Shazar, A. *Angew. Chem., Int. Ed. Engl.* **1993**, *32*, 1475−1477. (f) Protasiewicz, J. D.; Bianconi, P. A.; Williams, I. D.; Liu, S.; Rao, C. P.; Lippard, S. J. *Inorg. Chem.* **1992**, *31*, 4134−4142. (g) Bennett, M. A.; Bown, M.; Hockless, D. C. R. *Aust. J. Chem.* **2000**, *53*, 507−515.

(17) Evidence for electron richness of (η^6-arene)Mo(PR_3)$_3$ derivatives is provided by the observations that (i) the molybdenum center in [η^6-$C_6H_5C_6H_3$(Ph)-OH]Mo(PMe_3)$_3$ serves as a hydrogen bond acceptor such that the complex possesses an intramolecular Mo···H−OAr hydrogen bond,[a] (ii) (η^6-arene)-Mo(PR_3)$_3$ complexes may be doubly protonated to give [(η^6-arene)Mo-(PR_3)$_3H_2$]$^{2+}$,[b] and (iii) (η^6-arene)Mo(PR_3)$_3$ derivatives have low ionization potentials.[c,d] (a) Hascall, T.; Baik, M.-H.; Bridgewater, B. M.; Shin, J. H.; Churchill, D. G.; Friesner, R. A.; Parkin, G. *J. Chem. Soc., Chem. Commun.* **2002**, 2644−2645. (b) Green, M. L. H.; Mitchard, L. C.; Silverthorn, W. E. *J. Chem. Soc., Dalton Trans.* **1974**, 1361−1363. (c) Green, M. L. H.; Hughes, A. K.; Lincoln, P.; Martin-Polo, J. J.; Mountford, P.; Sella, A. Wong, L.-L.; Bandy, J. A.; Banks, T. W.; Prout, K.; Watkin, D. J. *J. Chem. Soc., Dalton Trans.* **1992**, 2063−2069. (d) Asirvatham, V. S.; Gruhn, N. E.; Lichtenberger, D. L.; Ashby, M. T. *Organometallics* **2000**, *19*, 2215−2227.

(18) Brookhart, M.; Cox, K.; Cloke, F. G. N.; Green, J. C.; Green, M. L. H.; Hare, P. M.; Bashkin, J.; Derome, A. E.; Grebenik, P. D. *J. Chem. Soc., Dalton Trans.* **1985**, 423−433.

(19) Oxidative addition of H_2 may, nevertheless, be induced photochemically to yield the dihydride complex (η^6-PhH)Mo(PMe_3)$_2H_2$. The latter compound, however, reacts with PMe_3 at room temperature to regenerate (η^6-PhH)Mo(PMe_3)$_3$, thereby indicating that oxidative addition of H_2 to (η^6-PhH)Mo(PMe_3)$_3$ is reversible.

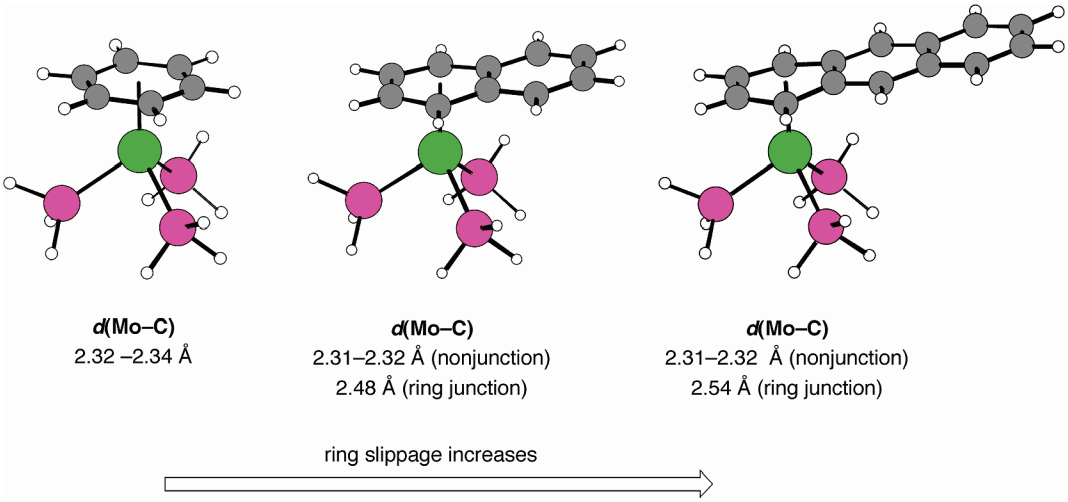

Figure 3. Geometry-optimized structures of (η^6-ArH)Mo(PH_3)$_3$.

The naphthalene complex (η^6-NpH)Mo(PMe_3)$_3$ is likewise inert towards H_2. It is, therefore, interesting that the anthracene derivative (η^6-AnH)Mo(PMe_3)$_3$ reacts readily with H_2 at room temperature to yield (η^4-AnH)Mo(PMe_3)$_3H_2$,[20] a transformation that is accompanied by an η^6-to-η^4 haptotropic shift of the anthracene ligand. The haptotropic shift is reversible, and removal of the H_2 atmosphere results in regeneration of (η^6-AnH)Mo(PMe_3)$_3$. The ability of the anthracene ligand to promote a transformation that is not observed for either the benzene or naphthalene counterparts may be described as an "anthracene effect".

In addition to forming an η^4-arene compound, anthracene is unique in that the ligand may be hydrogenated upon prolonged heating at 90 °C to liberate 1,2,3,4-tetrahydroanthracene.[21] Polycyclic arenes are typically easier to hydrogenate than monocyclic arenes, and the homogeneous hydrogenation of anthracene has been well documented.[8] The formation of 1,2,3,4-tetrahydroanthracene rather than 9,10-dihydroanthracene is indicative of a nonradical mechanism,[22] and thereby provides good evidence that hydrogenation occurs via (η^4-AnH)Mo(PMe_3)$_3H_2$.

2. Origin of the Naphthalene and Anthracene Effects. As noted above, ring fusion to benzene facilitates displacement of an arene. For example, the ease of substitution of the arene ligand of (η^6-ArH)Cr(CO)$_3$ by PR_3 increases in the sequence benzene < naphthalene < anthracene, a reaction that has been postulated to occur via an (η^4-ArH)Cr(CO)$_3$(PR_3) intermediate.[23] This trend has previously been rationalized in terms of the loss of resonance energy upon folding the arene from the planar geometry in (η^6-ArH)Cr(CO)$_3$ to that of the bent geometry in the proposed (η^4-ArH)Cr(CO)$_3$(PR_3) intermediate. Specifically, assuming that folding of the arene and adoption of an η^4-coordination mode causes a total loss of resonance energy for that ring only, the thermodynamics of the isomerization has been postulated to be a consequence of the variation in resonance energies of the individual arenes.[2c,23] Thus, since the incremental increase in resonance energy of "linear" fused arenes diminishes as the length of the arene increases,[24] the loss of resonance energy associated with the folding of the arene decreases in the sequence benzene > naphthalene > anthracene, and this variation has been proposed to rationalize the more facile displacement of the larger arene.[2c,23] While this simple argument, based only on energetic changes involving the arene ligand, could certainly rationalize the experimental observation that (η^6-AnH)Mo(PMe_3)$_3$ reacts more exothermically with H_2 than does either (η^6-PhH)Mo(PMe_3)$_3$ or (η^6-NpH)Mo(PMe_3)$_3$, we have performed density functional theory (DFT, B3LYP) calculations to procure a more detailed understanding of the influence of ring fusion on the haptotropic shifts of arene compounds.

The geometry-optimized structures of (η^6-ArH)Mo(PH_3)$_3$ and (η^4-ArH)Mo(PH_3)$_3H_2$ are illustrated in Figures 3 and 4, respectively, with selected bond lengths listed in Tables 2 and 3. Significantly, the calculated structures of (η^6-NpH)Mo(PH_3)$_3$ and (η^6-AnH)Mo(PH_3)$_3$ reproduce the "flat-slipped" coordination mode of the arenes in the experimentally derived structures of (η^6-NpH)Mo(PMe_3)$_3$ and (η^6-AnH)Mo(PMe_3)$_3$. In addition, the calculations also indicate that the arene ligands of the dihydrides (η^4-ArH)Mo(PH_3)$_3H_2$ exhibit an η^4-folded configuration. The variation in the C−C bond lengths associated with the coordinated arene rings of (η^6-ArH)Mo(PH_3)$_3$ and (η^4-ArH)-Mo(PH_3)$_3H_2$ is summarized in Figure 5. The most notable feature, which is exemplified for the benzene derivatives, is that the C−C bond lengths for the uncoordinated "double bonds" in the η^4-complexes are shorter than the corresponding values in the η^6-derivatives, while the adjacent bonds are longer.[25] These changes may be viewed in terms of the four carbon atoms involved in the η^4-coordination becoming "deconjugated" from

(20) A closely related η^4-cyclohexadiene compound, (η^4-C_6H_8)Mo(PMe_3)$_3H_2$, has been reported. See: Green, M. L. H.; Parkin, G. *J. Chem. Soc., Chem. Commun.* **1985**, 771−773.
(21) Mo(PMe_3)$_4H_4$ is the major molybdenum-containing product, but insoluble unidentified species are also formed.
(22) (a) Halpern, J. *Pure Appl. Chem.* **1979**, *51*, 2171−2182. (b) Landis, C. R.; Halpern, J. *Organometallics* **1983**, *2*, 840−842. (c) Grey, R. A.; Pez, G. P.; Wallo, A. *J. Am. Chem. Soc.* **1980**, *102*, 5948−5949. (d) Fordyce, W. A.; Wilczynski, R.; Halpern, J. *J. Organomet. Chem.* **1985**, *296*, 115−125. (e) Lynch, T. J.; Banah, M.; Kaesz, H. D.; Porter, C. R. *J. Org. Chem.* **1984**, *49*, 1266−1270.
(23) Zhang, S.; Shen, J. K.; Basolo, F.; Ju, T. D.; Lang, R. F.; Kiss, G.; Hoff, C. D. *Organometallics* **1994**, *13*, 3692−3702.
(24) Calculated resonance energies: benzene, 20.0 kcal mol^{-1}; naphthalene, 30.5 kcal mol^{-1}; and anthracene, 36.9 kcal mol^{-1}. See: Dewar, M. J.; Liano, C. D. *J. Am. Chem. Soc.* **1969**, *91*, 789−795.
(25) For representive papers describing the bonding variations in indenyl complexes, see: (a) Westcott, S. A.; Kakkar, A. K.; Stringer, G.; Taylor, N. J.; Marder, T. B. *J. Organomet. Chem.* **1990**, *394*, 777−794. (b) Kakkar, A. K.; Jones, S. F.; Taylor, N. J.; Collins, S.; Marder, T. B. *J. Chem. Soc., Chem. Commun.* **1989**, 1454−1456. (c) Trnka, T. M.; Bonanno, J. B.; Bridgewater, B. M.; Parkin, G. *Organometallics* **2001**, *20*, 3255−3264. (d) Cadierno, V.; Diez, J.; Gamasa, M. P.; Gimeno, J.; Lastra, E. *Coord. Chem. Rev.* **1999**, *193−195*, 147−205. (e) Calhorda, M. J.; Félix, V.; Veiros, L. F. *Coord. Chem. Rev.* **2002**, *230*, 49−64. (f) Reference 4.

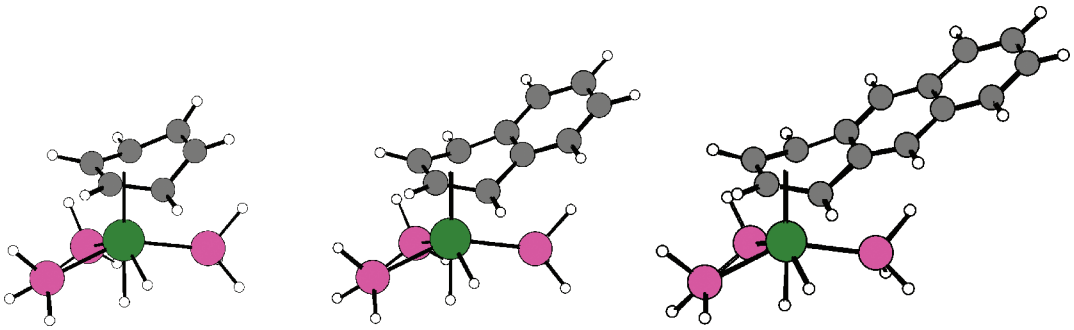

Figure 4. Geometry-optimized structures of (η^4-ArH)Mo(PH_3)$_3H_2$.

Table 2. Average Mo−C Bond Lengths for the Outer, Central, and Ring Junction Carbon Atoms of Geometry-Optimized (η^6-ArH)Mo(PH_3)$_3$

	benzene[a]	naphthalene	anthracene	1,2-$Me_2C_6H_4$
d(Mo−C_{outer})/Å	2.323	2.314	2.312	2.319
d(Mo−$C_{central}$)/Å	2.324	2.310	2.319	2.321
d(Mo−$C_{junction}$)/Å	2.325	2.475	2.533	2.354

[a] The outer, central, and junction designations for benzene are arbitrary.

Table 3. Average Mo−C Bond Lengths for the Outer, Central, and Ring Junction Carbon Atoms of Geometry-Optimized (η^4-ArH)Mo(PH_3)$_3H_2$

	benzene	naphthalene	anthracene
d(Mo−C_{outer})/Å	2.299	2.284	2.282
d(Mo−$C_{central}$)/Å	2.467	2.424	2.416
d(Mo−$C_{junction}$)/Å	3.265	3.220	3.190

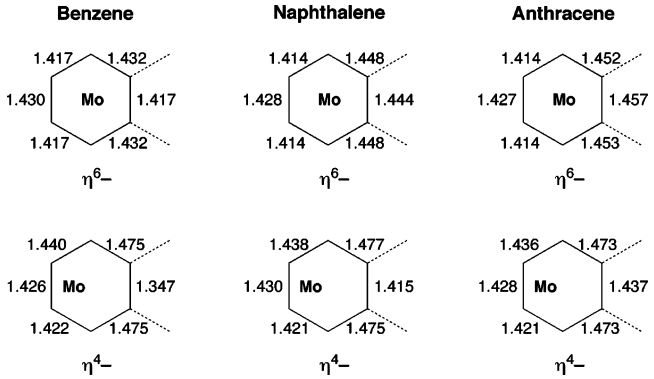

Figure 5. Variation of C−C bond lengths for the coordinated arene rings of (η^6-ArH)Mo(PH_3)$_3$ and (η^4-ArH)Mo(PH_3)$_3H_2$.

the remainder of the arene. In this regard, the C−C bond lengths of the uncoordinated "double bonds" in (η^4-ArH)Mo(PH_3)$_3H_2$ are marginally shorter than the corresponding calculated values in the free arenes (benzene, 1.397 Å; naphthalene, 1.432 Å; anthracene, 1.439 Å), while the respective C−C bond lengths in (η^6-AnH)Mo(PH_3)$_3$ are marginally longer.

The calculations are also in accord with the experimental observations concerned with the reactivity of (η^6-AnH)Mo(PMe_3)$_3$ towards H_2. Specifically, the calculated exothermicity of the oxidative addition of H_2 to (η^6-ArH)Mo(PH_3)$_3$ increases substantially in the sequence benzene (21.3 kcal mol^{-1}) < naphthalene (1.4 kcal mol^{-1}) < anthracene (−4.0 kcal mol^{-1}), as summarized in Table 4. To evaluate the proposal that the variation in the thermodynamics is dictated by a loss of resonance energy, we have calculated the energy required to fold the isolated arene (ΔE_{fold}) with the geometry in (η^6-ArH)-Mo(PH_3)$_3$ to that in (η^4-ArH)Mo(PH_3)$_3H_2$. As expected, the facility of folding the arene fragment does indeed increase in the sequence benzene (33.9 kcal mol^{-1}) < naphthalene (30.6 kcal mol^{-1}) < anthracene (26.8 kcal mol^{-1}), as summarized in Table 4 and Figure 6. However, the magnitude of the effect is sufficiently small that it does *not* determine the overall thermodynamics (Figure 7). Thus, the energy required to fold the arene decreases by only 7.1 kcal mol^{-1} from benzene to anthracene, whereas the exothermicity of the overall reaction increases by 25.3 kcal mol^{-1}. It is, therefore, evident that other factors are responsible for the observed effect, of which two are (i) energetic changes due to structural modifications of the [Mo(PH_3)$_3$] and [Mo(PH_3)$_3H_2$] moieties in the various arene complexes and (ii) variation of Mo−(η^6-ArH) and Mo−(η^4-ArH) bond energies; a simple thermodynamic cycle that incorporates these factors is illustrated in Figure 8.

Of these factors, the structural differences of the [Mo(PH_3)$_3$] and [Mo(PH_3)$_3H_2$] moieties in (η^6-ArH)Mo(PH_3)$_3$ and (η^4-ArH)-Mo(PH_3)$_3H_2$, respectively, are sufficiently small that they contribute little to the variation in overall thermodynamics, as illustrated by the similar energies associated with the oxidative addition of H_2 (ΔE_{+H_2}) to the various [Mo(PH_3)$_3$] fragments (Table 4 and Figure 9). The variation in overall thermodynamics does, however, correlate well with changes predicted by consideration of Mo−(η^6-ArH) and Mo−(η^4-ArH) bond energies (Figure 10). Specifically, the intrinsic "snap" Mo−(η^6-ArH) bond dissociation energies (BDEs) *decrease* in the sequence benzene (67.1 kcal mol^{-1}) > naphthalene (62.2 kcal mol^{-1}) ≈ anthracene (64.0 kcal mol^{-1}),[26] whereas the Mo−(η^4-ArH) BDEs exhibit the opposite trend and *increase* in the sequence benzene (64.4 kcal mol^{-1}) < naphthalene (77.5 kcal mol^{-1}) < anthracene (82.1 kcal mol^{-1}). As a result of these opposing trends, of which the latter is dominant, the oxidative addition of H_2 becomes more exothermic in the sequence benzene < naphthalene < anthracene. In this regard, it is pertinent to note that a recent analysis of the indenyl effect has concluded that the more facile η^5-to-η^3 haptotropic shift is a consequence of (i) the M−(η^3-Ind) bond being stronger than the M−(η^3-Cp) bond and (ii) the M−(η^5-Ind) bond being weaker than the M−(η^5-Cp) bond.[27]

The key to understanding the influence of ring fusion on η^6-to-η^4 haptotropic shifts of arene ligands is, therefore, concerned with why the Mo−(η^6-ArH) and Mo−(η^4-ArH) bond energies

(26) This trend in M−(η^6-ArH) BDEs has been observed experimentally. For example, the Cr−arene bond energy in (η^6-PhH)Cr(CO)$_3$ is respectively 4.9 and 5.9 kcal mol^{-1} stronger than that in (η^6-NpH)Cr(CO)$_3$ and (η^6-AnH)Cr(CO)$_3$. See ref 23.

(27) (a) Veiros, L. F. *Organometallics* **2000**, *19*, 3127−3136. (b) Calhorda, M. J.; Romão, C. C.; Veiros, L. F. *Chem. Eur. J.* **2002**, *8*, 868−875.

Table 4. DFT-Calculated Energy Values (H^{SCF}) Pertaining to the Thermodynamic Cycle for Oxidative Addition of H_2 to (η^6-AnH)Mo(PH_3)$_3$ (Values in kcal mol^{-1})

		benzene	naphthalene	anthracene
(η^6-ArH)Mo(PH_3)$_3$ + H_2 → (η^4-ArH)Mo(PH_3)$_3H_2$	$\Delta E_{overall}$[a]	21.27	1.37	−3.99
(η^6-ArH)Mo(PH_3)$_3$ → ArH[η^6-geom] + [Mo(PH_3)$_3$]^{singlet}	BDE[Mo−(η^6-ArH)]	67.07	62.22	64.00
ArH[η^6-geom] → ArH[η^4-geom]	ΔE_{fold}	33.87	30.55	26.83
[Mo(PH_3)$_3$]^{singlet} + H_2 → [Mo(PH_3)$_3H_2$]^{singlet}	ΔE_{+H_2}	−15.28	−13.90	−12.70
(η^4-ArH)Mo(PH_3)$_3H_2$ → ArH[η^4-geom] + [Mo(PH_3)$_3H_2$]^{singlet}	−BDE[Mo−(η^4-ArH)]	−64.39	−77.50	−82.12

[a] $\Delta E_{overall} = \{BDE[Mo-(\eta^6\text{-ArH})] - BDE[Mo-(\eta^4\text{-ArH})]\} + \Delta E_{fold} + \Delta E_{+H_2}$.

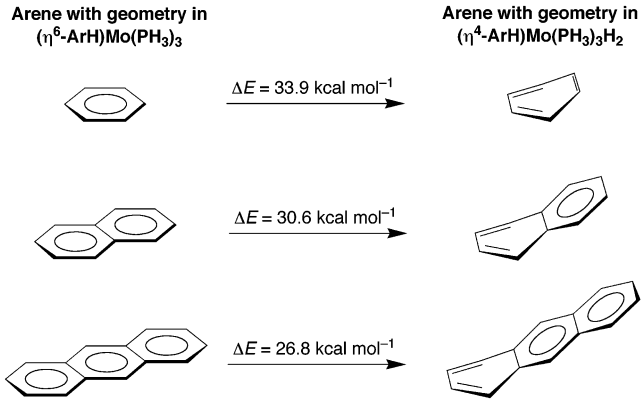

Figure 6. Energy changes for folding an isolated arene with the geometry in (η^6-ArH)Mo(PH_3)$_3$ to that in (η^4-ArH)Mo(PH_3)$_3H_2$.

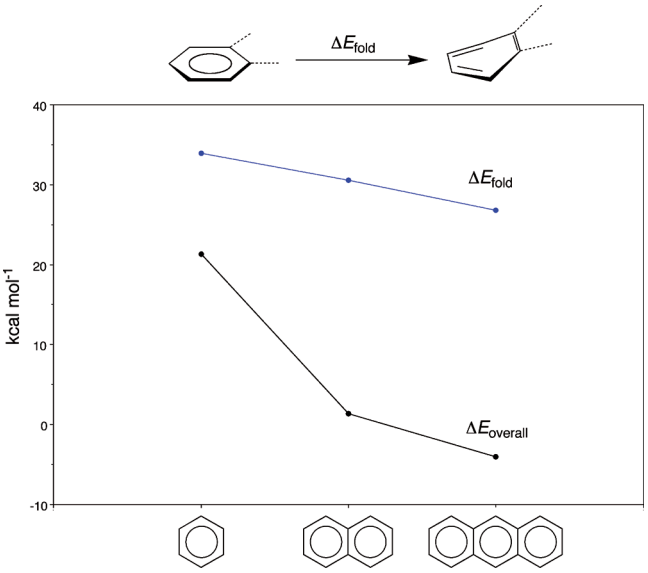

Figure 7. Comparison of the energy required to fold an isolated arene with the overall energy of oxidative addition to (η^6-ArH)Mo(PH_3)$_3$.

exhibit opposing trends. It is, therefore, pertinent to discuss the nature of the bonding in these complexes. In this regard, the transition metal−(η^6-arene) interaction has been the subject of many theoretical calculations, and on this basis it is generally recognized that π-donation from the arene highest occupied molecular orbital (HOMO) to an appropriate metal d_π-orbital provides an important component that is supplemented by a δ-back-bonding interaction with the arene lowest unoccupied molecular orbital (LUMO);[28,29] a molecular orbital diagram for (η^6-PhH)Mo(PH_3)$_3$ which illustrates these interactions is shown in Figure 11. Focusing on the π-donor interaction, the effect of ring fusion on Mo−(η^6-ArH) bond energies may be traced to

(28) Muetterties, E. L.; Bleeke, J. R.; Wucherer, E. J.; Albright, T. A. *Chem. Rev.* **1982**, *82*, 499−525.

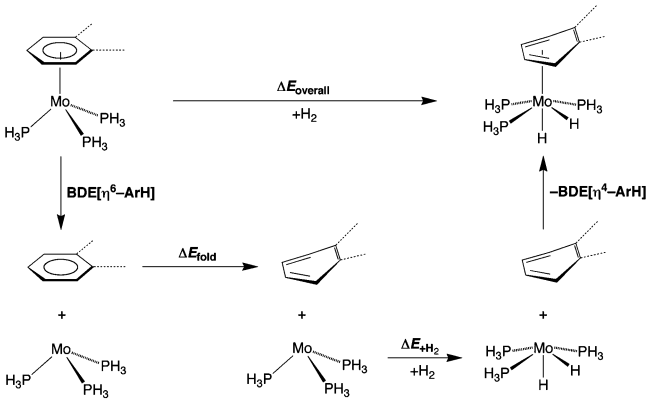

Figure 8. Thermodynamic cycle for oxidative addition of H_2 to (η^6-ArH)-Mo(PH_3)$_3$ decomposed in terms of intrinsic "snap" Mo−(η^6-ArH) and Mo−(η^4-ArH) bond energies, the energy required to fold the arene (ΔE_{fold}), and the energy associated with the oxidative addition of H_2 (ΔE_{+H_2}) to the various [Mo(PH_3)$_3$] fragments with the geometries in (η^6-ArH)Mo(PH_3)$_3$.

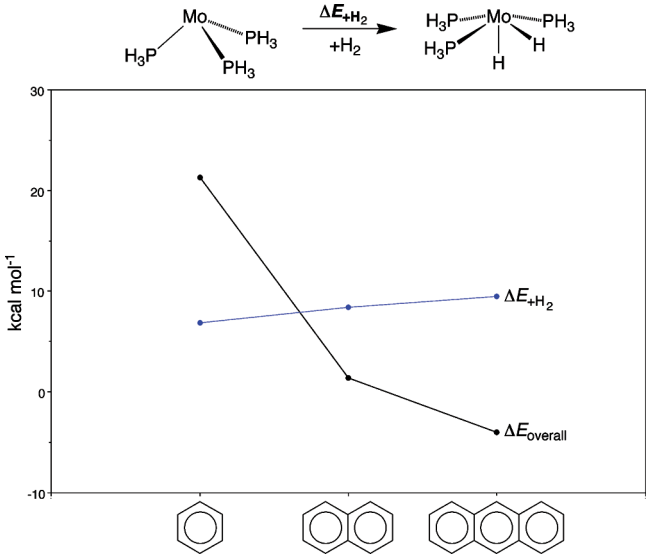

Figure 9. Comparison of the energy associated with the oxidative addition of H_2 (ΔE_{+H_2}) to the various [Mo(PH_3)$_3$] fragments with the overall energy of oxidative addition to (η^6-ArH)Mo(PH_3)$_3$.

the different nature of the HOMOs of the various arenes (Figure 12). For benzene, the HOMO is a doubly degenerate e_{1g} orbital, the symmetry of which enforces symmetric η^6-coordination. In

(29) For calculations on (η^6-arene)ML_3 complexes, see: (a) Howell, J. A. S.; Ashford, N. F.; Dixon, D. T.; Kola, J. C.; Albright, T. A.; Kwang, S. K. *Organometallics* **1991**, *10*, 1852−1864. (b) Albright, T. A.; Hofmann, P.; Hoffmann, R.; Lillya, C. P.; Dobosh, P. A. *J. Am. Chem. Soc.* **1983**, *105*, 3396−3411. (c) Byers, B. P.; Hall, M. B. *Organometallics* **1987**, *6*, 2319−2325. (d) Rogers, R. D.; Atwood, J. L.; Albright, T. A.; Lee, W. A.; Rausch, M. D. *Organometallics* **1984**, *3*, 263−270. (e) Albright, T. A.; Hofmann, P.; Hoffmann, R. *J. Am. Chem. Soc.* **1977**, *99*, 7546−7557. (f) Albright, T. A.; Carpenter, B. K. *Inorg. Chem.* **1980**, *19*, 3092−3097. (g) Cohen, R.; Weitz, E.; Martin, J. M. L.; Ratner, M. A. *Organometallics* **2004**, *23*, 2315−2325. (h) Albright, T. A. *Acc. Chem. Res.* **1982**, *15*, 149−155. (i) Reference 17d.

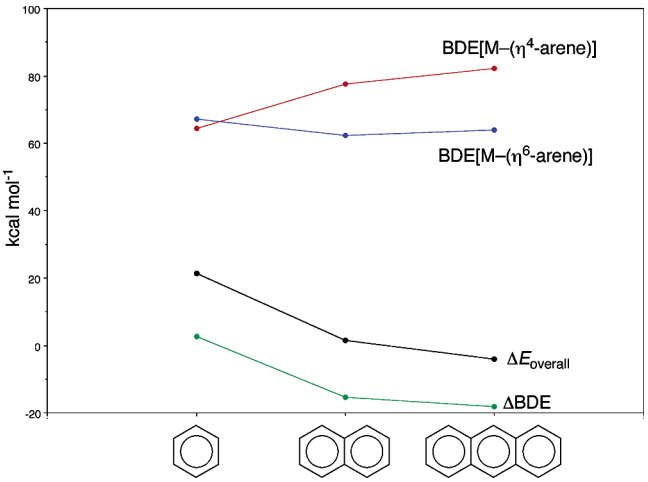

Figure 10. Variation of intrinsic "snap" Mo−(η^6-ArH) and Mo−(η^4-ArH) bond energies. Note that the difference in bond energies (ΔBDE) correlates well with the overall energy of oxidative addition to (η^6-ArH)Mo(PH_3)$_3$.

contrast, the HOMO of naphthalene is asymmetric with respect to each six-membered ring, with no p-orbital coefficient on carbon atoms of the ring junction.[28] As such, the most efficient overlap is achieved if the naphthalene ligand slips to maximize the interaction with the four nonjunction atoms. Thus, while the benzene ring of (η^6-PhH)Mo(PH_3)$_3$ is coordinated symmetrically to molybdenum, with Mo−C bond lengths in the range 2.32−2.34 Å, the naphthalene ring of (η^6-NpH)Mo(PH_3)$_3$ is displaced and approaches a "flat" η^4-coordination mode (see Figure 3 and Table 2). For example, the Mo−C distances of the nonjunction atoms of (η^6-NpH)Mo(PH_3)$_3$ (2.31−2.32 Å) are distinctly shorter than those of the ring junction (2.48 Å). Evidence that this displacement is undoubtedly an electronic and not steric effect is provided by the observation that the 1,2-dimethylbenzene ligand in (η^6-1,2-$Me_2C_6H_4$)Mo(PH_3)$_3$ exhibits little displacement from symmetric η^6-coordination (2.32−2.35 Å; Table 2). The displacement of the naphthalene ligand of (η^6-NpH)Mo(PH_3)$_3$ from symmetric coordination is in accord with a reduced bonding interaction compared to that of benzene in (η^6-PhH)Mo(PH_3)$_3$.

Whereas the HOMO of naphthalene has a node on the carbon atoms of the ring junction, the corresponding carbon atoms of anthracene have a small contribution that is out-of-phase[30] with respect to the metal d_π-orbital and thereby further reduces the π-bonding interaction. The anthracene ligand, therefore, slips to a further degree than does the naphthalene ligand, such that the Mo−C distances for the ring junction increase to 2.54 Å. The Mo−(η^6-AnH) interaction is, however, slightly stronger than the Mo−(η^6-NpH) bond, presumably because anthracene is a better acceptor[31] and back-bonding is more efficient (vide infra).

The stability of (η^4-ArH)Mo(PH_3)$_3H_2$ depends critically on the energy of the metal−arene antibonding orbital derived by interaction of occupied arene and metal orbitals. The energy of this occupied metal−arene antibonding orbital is reduced substantially via a back-bonding interaction with the arene LUMO, an interaction that becomes significant upon folding the arene and slipping to an η^4-coordination mode (Figure 13).

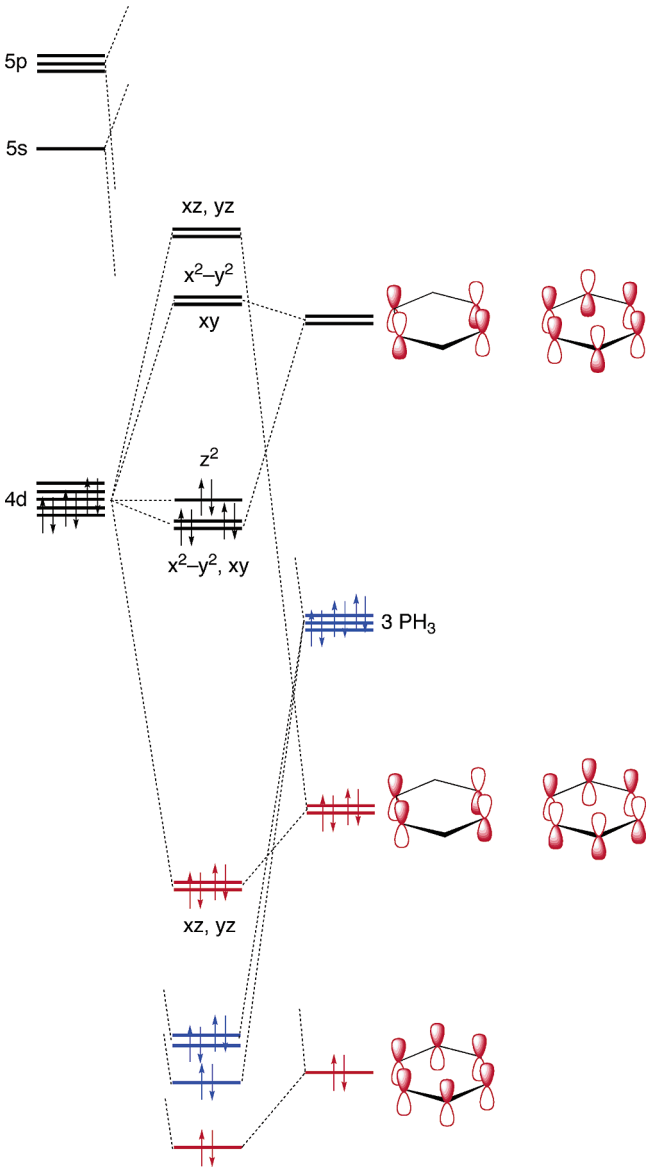

Figure 11. Qualitative molecular orbital diagram for (η^6-PhH)Mo(PH_3)$_3$ (the *z*-axis is defined as the Mo−benzene centroid).

In essence, the d_{xz} orbital of (η^4-ArH)Mo(PH_3)$_3H_2$ (with *x* representing the slip direction) interacts not only with an occupied arene orbital but also with the arene LUMO,[32] resulting in a standard three-orbital interaction pattern. The energy of the occupied midlevel orbital is determined by the relative energy of the arene LUMO, a simple estimate of which is provided by the HOMO−LUMO gap of (η^6-ArH)Mo(PH_3)$_3$, and decreases in the sequence benzene (4.4 eV) > naphthalene (3.3 eV) > anthracene (2.7 eV).[33] This trend is consistent with an increased back-bonding interaction and hence a corresponding increase in Mo−(η^4-ArH) bond energy across the series benzene < naphthalene < anthracene. While slipping alone provides a mechanism by which the arene LUMO may participate in a π-back-bonding interaction, the arene ligand of (η^4-ArH)Mo(PH_3)$_3H_2$ folds in order to stabilize the midlevel component of the three-orbital interaction by minimizing the antibonding

(30) Zilberg, S.; Haas, Y.; Shaik, S. *J. Phys. Chem.* **1995**, *99*, 16558−16565.
(31) For example, the HOMO−LUMO gaps of the free arenes are as follow: benzene, 6.64 eV; naphthalene, 4.74 eV; and anthracene, 3.54 eV (B3LYP and cc-pVTZ(-f) basis set).
(32) Note that the arene LUMO also participates in a δ-back-bonding interaction with the metal center.
(33) The HOMO−LUMO gaps of the free arenes exhibit the same trend. See ref 31.

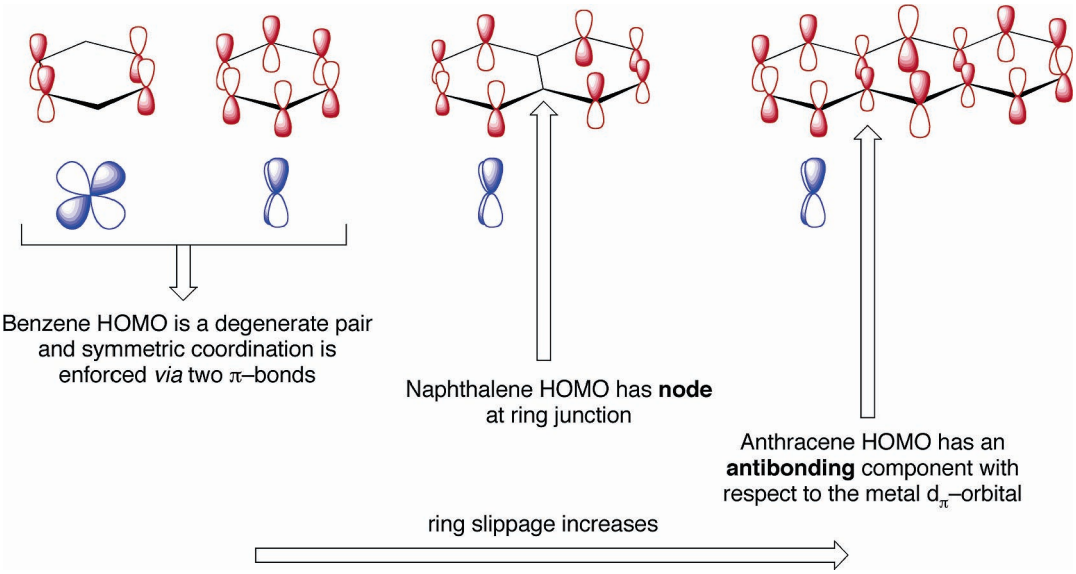

Figure 12. Interaction of the various arene HOMOs with a d_π-orbital. The degenerate nature of the benzene HOMO enforces symmetric coordination, while the asymmetric nature of the naphthalene and anthracene HOMOs promotes a ring-slip in order to maximize the d_π-interaction with the nonjunction carbon atoms.

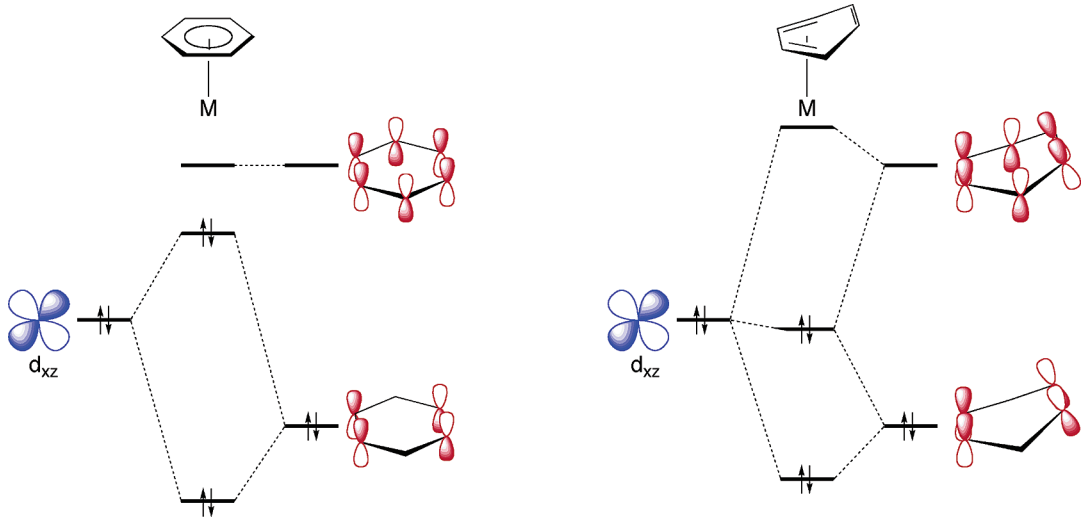

Figure 13. Simplified illustration of the role of the benzene LUMO in stabilizing an occupied M−benzene antibonding d_π-orbital upon displacing the benzene ligand along the *x*-axis (for clarity, the interaction between only one component of the doubly degenerate LUMO is illustrated). For an η^6-benzene complex (left), the d_{xz} orbital cannot interact with the benzene LUMO, and if the d_{xz} orbital is occupied (as it is in a "20-electron" (η^4-ArH)Mo$(PH_3)_3H_2$ complex), the interaction with the occupied benzene orbital is unfavorable. However, the reduced symmetry associated with η^4-benzene coordination (right) enables the benzene LUMO to stabilize the occupied antibonding component of the filled−filled interaction between the occupied d_{xz} orbital and occupied benzene orbital. As such, a "20-electron" complex adopts an η^4-coordination mode.

interaction between d_{xz} and the orbital component on the two nonbonded atoms, as illustrated in Figure 14. The observation that the M−(η^3-Ind) bond is calculated to be stronger than the M−(η^3-Cp) bond has been rationalized in similar terms, with the HOMO being less antibonding for the indenyl derivative.[27]

A more quantitative analysis of the back-bonding interactions in (η^6-ArH)Mo$(PH_3)_3$ and (η^4-ArH)Mo$(PH_3)_3H_2$ has been obtained by evaluation of the energy difference and overlap between the occupied metal-based orbitals and unoccupied arene orbitals, as summarized in Tables 5 and 6. Examination of these data indicates that the back-bonding interaction, as crudely evaluated by the overlap/ΔE ratio, increases in the sequence benzene < naphthalene < anthracene for both (η^6-ArH)Mo$(PH_3)_3$ and (η^4-ArH)Mo$(PH_3)_3H_2$, but the interaction is much more significant for the latter because the energy gap is considerably smaller. Thus, to a first approximation, the variation in the exothermicity of the oxidative addition of H_2 to (η^6-ArH)Mo$(PH_3)_3$ may be rationalized in terms of the differing back-bonding interactions within (η^4-ArH)Mo$(PH_3)_3H_2$.

Experimental Details

General Considerations. All manipulations were performed using a combination of dry glovebox, high-vacuum, and Schlenk techniques under an argon atmosphere.[34] Solvents were purified and degassed by standard procedures. Mo$(PMe_3)_6$ was prepared by the literature method.[35]

^{1}H and ^{13}C NMR spectra were measured on Bruker 300wb DRX, Bruker Avance 400 DRX, and Bruker Avance 500 DMX spectrometers. Chemical shifts are reported in ppm relative to $SiMe_4$ ($\delta = 0$) and were referenced internally with respect to the protio solvent impurity ($\delta = 7.15$ for C_6D_5H and $\delta = 2.09$ for $C_6D_5CD_2H$) and the ^{13}C

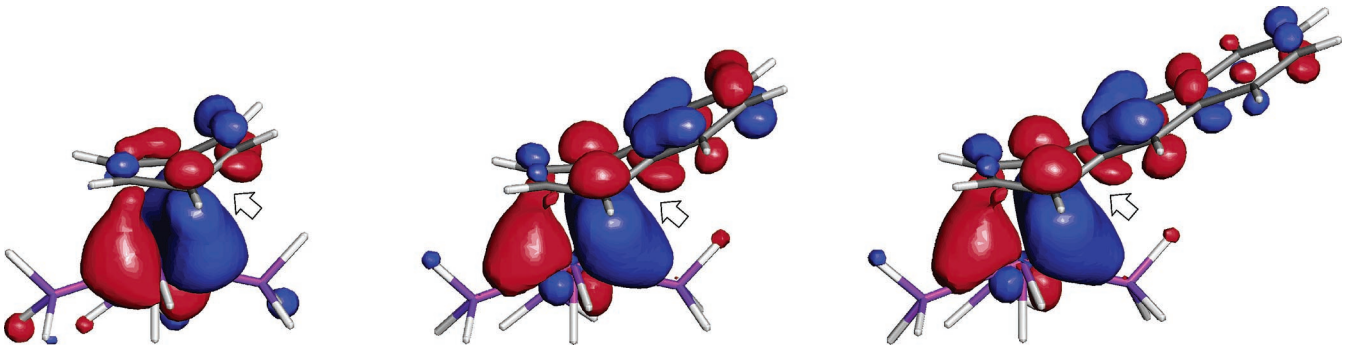

Figure 14. Occupied midlevel component of the three-orbital interaction for (η^4-ArH)Mo(PH_3)$_3H_2$. The arrow indicates the out-of-phase component with the d_{xz} orbital that promotes folding of the arene in these complexes.

Table 5. Analysis of the Principal Back-Bonding Interactions in (η^6-ArH)Mo(PH_3)$_3$

	E/eV				
	Mo(PH_3)$_3$ (occ)	arene (unocc)	ΔE/ eV	overlap (au)	overlap/ ΔE
benzene[a]	−4.380	−2.262	2.118	1.22×10^{-1}	0.06
	−4.376	−2.260	2.116	1.22×10^{-1}	0.06
naphthalene	−4.351	−3.120	1.231	1.50×10^{-1}	0.12
anthracene	−4.328	3.662	0.666	1.23×10^{-1}	0.18

[a] In contrast to the naphthalene and anthracene derivatives, the two back-bonding interactions in (η^6-ArH)Mo(PH_3)$_3$ are almost degenerate due to the higher symmetry.

Table 6. Analysis of the Principal Back-Bonding Interactions in (η^4-ArH)Mo(PH_3)$_3H_2$

	E/eV				
	Mo(PH_3)$_3H_2$ (occ)	arene (unocc)	ΔE/ eV	overlap (au)	overlap/ ΔE
benzene	−4.357	−3.339	1.018	2.21×10^{-1}	0.22
naphthalene	−4.312	−3.719	0.593	2.21×10^{-1}	0.37
anthracene	−4.264	−3.979	0.285	2.07×10^{-1}	0.73

resonances (δ = 128.0 for C_6D_6), respectively. ^{31}P NMR spectra were referenced relative to 85% H_3PO_4 (δ = 0) using P(OMe)$_3$ as an external reference (δ = 141.0). All coupling constants are reported in hertz. Variable-temperature T_1 measurements were made at 300 MHz using the inversion recovery method. IR spectra were recorded on a Perkin-Elmer Paragon 1000 spectrophotometer.

Synthesis of (η^6-PhH)Mo(PMe_3)$_3$. A suspension of Mo(PMe_3)$_6$ (50 mg, 0.09 mmol) in benzene (2 mL) was heated at 120 °C for 1 day, after which period the volatile components were removed in vacuo. The solid residue was extracted into benzene (1 mL) and filtered, and the filtrate was lyophilized to give (η^6-PhH)Mo(PMe_3)$_3$ as a dark brown solid (30 mg, 82% yield). ^{1}H NMR data (C_6D_6): 1.18 [br, 9 Me of 3 P(CH_3)$_3$], 3.69 [m, 6 H of C_6H_6]. ^{13}C{^{1}H} NMR data (C_6D_6): 27.2 [m, 9 Me of 3 P(CH_3)$_3$], 71.8 [s, 6 CH of C_6H_6]. ^{31}P{^{1}H} NMR data (C_6D_6): 3.3 [br, 3 P of 3 P(CH_3)$_3$]. IR data (KBr disk, cm^{-1}): 3045 (m), 3024 (m), 2957 (vs), 2895 (vs), 2800 (w), 1418 (m), 1287 (w), 1269 (s), 946 (vs), 926 (vs), 836 (m), 758 (m), 690 (s), 649 (vs), 594 (w).

Synthesis of (η^6-NpH)Mo(PMe_3)$_3$. A mixture of Mo(PMe_3)$_6$ (55 mg, 0.10 mmol) and naphthalene (13 mg, 0.10 mmol) in cyclohexane (1 mL) was heated at 140 °C for 2 days, after which period the volatile components were removed in vacuo. The solid residue was extracted into pentane (1 mL) and filtered, and the volatile components were removed from the filtrate in vacuo to give (η^6-NpH)Mo(PMe_3)$_3$ as a dark brown solid (18 mg, 40% yield). ^{1}H NMR data (C_6D_6): 1.11 [br, 9 Me of 3 P(CH_3)$_3$], 3.71 [br, 2 H of $C_{10}H_8$], 4.32 [br, 2 H of $C_{10}H_8$], 6.70 [m, $^3J_{H-H}$ = 3, 2 H of $C_{10}H_8$], 7.21 [m, $^3J_{H-H}$ = 3, 2 H of $C_{10}H_8$]. ^{13}C{^{1}H} NMR data (C_6D_6): 26.0 [m, 9 Me of 3 P(CH_3)$_3$], 68.5 [s, 2 CH of $C_{10}H_8$], 72.5 [s, 2 CH of $C_{10}H_8$], 97.1 [s, 2 C of $C_{10}H_8$], 121.3 [s, 2 CH of $C_{10}H_8$], 129.2 [s, 2 CH of $C_{10}H_8$]. ^{31}P{^{1}H} NMR data (C_6D_6): 4.8 [br, 3 P of 3 P(CH_3)$_3$]. IR data (KBr disk, cm^{-1}): 3044 (w), 2985 (w), 2956 (s), 2895 (vs), 2797 (w), 2366 (vw), 2345 (vw), 1419 (m), 1412 (m), 1346 (m), 1286 (m), 1269 (s), 1237 (w), 1078 (w), 985 (w), 944 (vs), 928 (vs), 840 (s), 799 (m), 786 (m), 773 (m), 738 (s), 701 (m), 688 (s), 658 (s), 650 (s), 620 (m), 570 (w).

Synthesis of (η^6-AnH)Mo(PMe_3)$_3$. A mixture of Mo(PMe_3)$_6$ (55 mg, 0.10 mmol) and anthracene (18 mg, 0.10 mmol) in cyclohexane (2 mL) was heated at 140 °C for 4 days, after which period the volatile components were removed in vacuo. The solid residue was extracted into pentane (1 mL) and filtered, and the solvent was removed in vacuo. The residue was dissolved in benzene and lyophilized to give (η^6-AnH)-Mo(PMe_3)$_3$ as a green solid (30 mg, 60% yield). ^{1}H NMR spectroscopy indicates that the crude sample contains ca. 15% residual anthracene. Crystals suitable for X-ray diffraction were grown from pentane by slow evaporation. ^{1}H NMR data (C_6D_6): 1.17 [d, $^2J_{P-H}$ = 4, 9 Me of 3 P(CH_3)$_3$], 4.00 [d, $^3J_{H-H}$ = 4, 2 H of $C_{14}H_{10}$], 4.59 [s, 2 H of $C_{14}H_{10}$], 7.03 [m, 2 H of $C_{14}H_{10}$], 7.54 [s, 2 H of $C_{14}H_{10}$], 7.57 [m, 2 H of $C_{14}H_{10}$]. ^{13}C{^{1}H} NMR data (C_6D_6): 27.2 [s, 9 Me of 3 P(CH_3)$_3$], 67.6 [s, 2 CH of $C_{14}H_{10}$], 74.8 [s, 2 CH of $C_{14}H_{10}$], 104.3 [s, 2 C of $C_{14}H_{10}$], 121.6 [s, 2 CH of $C_{14}H_{10}$], 122.5 [s, 2 CH of $C_{14}H_{10}$], 126.4 [s, 2 CH of $C_{14}H_{10}$], 130.7 [s, 2 C of $C_{14}H_{10}$]. ^{31}P{^{1}H} NMR data (C_6D_6): 7.1 [br, 2 P of 3 P(CH_3)$_3$], 9.3 [br, 1 P of 3 P(CH_3)$_3$]. IR data (KBr disk, cm^{-1}): 3048 (m), 2959 (vs), 2896 (vs), 2799 (m), 1609 (w), 1570 (w), 1454 (w), 1414 (s), 1327 (m), 1288 (m), 1269 (s), 1238 (m), 1120 (w), 944 (vs), 927 (vs), 836 (s), 687 (s), 649 (s).

Reactivity of (η^6-PhH)Mo(PMe_3)$_3$ towards H_2. A solution of (η^6-PhH)Mo(PMe_3)$_3$ (5 mg) in C_6D_6 (0.5 mL) in an NMR tube was saturated with H_2 (1 atm) and heated at 80 °C for 2 days. The sample was monitored by ^{1}H NMR spectroscopy, thereby demonstrating that there was no reaction between (η^6-PhH)Mo(PMe_3)$_3$ and H_2. Upon heating at 120 °C for 1 day, the sample was observed to decompose with the formation of a black precipitate.

Reactivity of (η^6-NpH)Mo(PMe_3)$_3$ towards H_2. A solution of (η^6-NpH)Mo(PMe_3)$_3$ (3 mg) in C_6D_6 (0.5 mL) in an NMR tube was saturated with H_2 (1 atm) and heated at 80 °C for 2 days. The sample was monitored by ^{1}H NMR spectroscopy, thereby demonstrating that there was no reaction between (η^6-NpH)Mo(PMe_3)$_3$ and H_2. Upon heating at 120 °C for 1 day, the sample was observed to decompose with the formation of a black precipitate.

Reactivity of (η^6-AnH)Mo(PMe_3)$_3$ towards H_2. (a) Generation of (η^4-AnH)Mo(PMe_3)$_3H_2$. A solution of (η^6-AnH)Mo(PMe_3)$_3$ (5 mg)

(34) (a) McNally, J. P.; Leong, V. S.; Cooper, N. J. In *Experimental Organometallic Chemistry*; Wayda, A. L., Darensbourg, M. Y., Eds.; American Chemical Society: Washington, DC, 1987; Chapter 2, pp 6−23. (b) Burger, B. J.; Bercaw, J. E. In *Experimental Organometallic Chemistry*; Wayda, A. L., Darensbourg, M. Y., Eds.; American Chemical Society: Washington, DC, 1987; Chapter 4, pp 79−98. (c) Shriver, D. F.; Drezdzon, M. A. *The Manipulation of Air-Sensitive Compounds*, 2nd ed.; Wiley-Interscience: New York, 1986.

(35) (a) Murphy, V. J.; Parkin, G. *J. Am. Chem. Soc.* **1995**, *117*, 3522−3528. (b) Hascall, T. Ph.D. Thesis, Columbia University, New York, 1999.

in C_6D_6 (1 mL) in an NMR tube was saturated with H_2 (1 atm). The sample was monitored by ^1H and ^{31}P NMR spectroscopy, thereby demonstrating the formation of (η^4-AnH)Mo(PMe_3)$_3H_2$ over the period of 1 day at room temperature. Low-temperature ^1H NMR spectroscopy at −70 °C reveals two conformations of (η^4-AnH)Mo(PMe_3)$_3H_2$ with a ca. 5:1 ratio. ^1H NMR data (C_6D_6 at 25 °C): −4 [very broad, 2 MoH], 1.01 [d, $^2J_{P-H}$ = 7, 9 Me of 3 P(CH_3)$_3$], 2.76 [br, 2 H of $C_{14}H_{10}$], 4.78 [br, 2 H of $C_{14}H_{10}$], 6.80 [s, 2 H of $C_{14}H_{10}$], 7.12 [m, 2 H of $C_{14}H_{10}$], 7.43 [m, 2 H of $C_{14}H_{10}$]. ^1H NMR data ($C_6D_5CD_3$ at 90 °C, hydride region only): −3.87 [q, $^2J_{P-H}$ = 44, 2 H of MoH_2]. ^1H NMR data ($C_6D_5CD_3$ at −70 °C, hydride region only): −3.99 [tt, $^2J_{P-H}$ = 40, $^2J_{P-H}$ = 9, $^1J_{H-H}$ = 9, 1 H of MoH_2], −2.47 [m, $^2J_{P-H}$ = 65, $^2J_{P-H}$ = 42, $^2J_{P-H}$ = 32, $^1J_{H-H}$ = 9, 1 H of MoH_2] (major species); −8.49 [tt, $^2J_{P-H}$ = 56, $^2J_{P-H}$ = 10, $^1J_{H-H}$ = 10, 1 H of MoH_2], −3.71 [m, 1H of MoH_2] (minor species). The T_1 minimum values of the hydride signals of the major species in toluene-d_8 are 210 ms (δ −3.99 ppm) and 199 ms (δ −2.47 ppm) at 300 MHz and −60 °C, consistent with a dihydride, rather than dihydrogen, structure. $^{31}P\{^1H\}$ NMR data (C_6D_6 at 25 °C): 3.4 [s, 3 P of 3 $P(CH_3)_3$]. $^{31}P\{^1H\}$ NMR data ($C_6D_5CD_3$ at −70 °C), two conformations are observed: ABC pattern 5.3 [P_A, $^2J_{P-P}$ = 11, $^2J_{P-P}$ = 24, 1 P of 3 $P(CH_3)_3$], 6.1 [P_B, $^2J_{P-P}$ = 11, $^2J_{P-P}$ = 34, 1 P of 3 $P(CH_3)_3$], and 15.9 [P_C, $^2J_{P-P}$ = 24, $^2J_{P-P}$ = 34, 1 P of 3 $P(CH_3)_3$] (major species); −2.2 [t, $^2J_{P-P}$ = 15, 1 P of 3 $P(CH_3)_3$] and 5.7 [d, $^2J_{P-P}$ = 15, 2 P of 3 $P(CH_3)_3$] (minor species). IR data (KBr disk, cm^{-1}): 3049 (s), 2964 (vs), 2900 (vs), 2801 (w), 1783 (m), 1727 (m) [ν(Mo−H)], 1618 (m)**, 1464 (s), 1407 (s), 1315 (m)**, 1297 (m), 1274 (s), 1233 (m), 1145 (m)*, 938 (vs), 881 (vs)*, 853 (s), 738 (s), 722 (vs), 663 (s), 471 (s); absorptions labeled * are present in (η^6-AnH)Mo(PMe_3)$_3$, while those labeled ** are present in anthracene.

(b) Reductive Elimination of H_2 from (η^4-AnH)Mo(PMe_3)$_3H_2$. A sample of (η^4-AnH)Mo(PMe_3)$_3H_2$ in C_6D_6 (0.5 mL), prepared as described above, was frozen and evacuated to remove the H_2 atmosphere. The sample was allowed to warm to room temperature and was monitored by ^1H NMR spectroscopy, thereby demonstrating that (η^4-AnH)Mo(PMe_3)$_3H_2$ converted to an equilibrium mixture with (η^6-AnH)Mo(PMe_3)$_3$ and H_2 over a period of 1 day.

(c) Hydrogenation of (η^4-AnH)Mo(PMe_3)$_3H_2$ in C_6D_6. A sample of (η^4-AnH)Mo(PMe_3)$_3H_2$ in C_6D_6 (0.5 mL), prepared as described above in the presence of H_2 (1 atm), was heated at 90 °C for one week and monitored by ^1H NMR spectroscopy, thereby demonstrating the conversion to 1,2,3,4-tetrahydroanthracene[36] (ca. 67% yield based on (η^6-AnH)Mo(PMe_3)$_3$ using mesitylene as an internal standard); a small quantity of 9,10-dihydroanthracene (ca. 4% yield)[37] is also obtained. The reaction is accompanied by liberation of anthracene (ca. 29% yield) and the formation of Mo(PMe_3)$_4H_4$, (η^6-PhH-d_6)Mo(PMe_3)$_3$, and a small amount of unidentified precipitate. The ratio of Mo(PMe_3)$_4H_4$:(η^6-PhH-d_6)Mo(PMe_3)$_3$ decreases over the course of the reaction as Mo(PMe_3)$_4H_4$ converts to (η^6-PhH-d_6)Mo(PMe_3)$_3$ (ca. 95% yield after one week).

(d) Hydrogenation of (η^4-AnH)Mo(PMe_3)$_3H_2$ in C_6D_{12}. A sample of (η^6-AnH)Mo(PMe_3)$_3$ in C_6D_{12} (0.5 mL) was treated with PMe_3 (ca. 30 μL) and H_2 (1 atm) to generate (η^4-AnH)Mo(PMe_3)$_3H_2$. The sample was heated at 80 °C for 25 days and analyzed by ^1H NMR spectroscopy, thereby demonstrating the conversion to 1,2,3,4-tetrahydroanthracene (ca. 78% yield based on (η^6-AnH)Mo(PMe_3)$_3$ using mesitylene as an internal standard); in contrast to the reaction in C_6D_6, 9,10-dihydroanthracene was not observed and the amount of liberated anthracene was reduced to ca. 15%. The reaction was accompanied by the formation of a black precipitate and Mo(PMe_3)$_4H_4$ (ca. 14% yield).

X-ray Structure Determinations. X-ray diffraction data for (η^6-NpH)Mo(PMe_3)$_3$ and (η^6-AnH)Mo(PMe_3)$_3$ were collected on a Bruker P4 diffractometer equipped with a SMART CCD detector; crystal data, data collection, and refinement parameters are summarized in Table 7. The structures were solved using direct methods and standard difference map techniques and were refined by full-matrix least-squares procedures on F^2 with SHELXTL (version 6.10).[38]

Table 7. Crystal Data, Data Collection, and Refinement Parameters

	(η^6-NpH)Mo(PMe_3)$_3$	(η^6-AnH)Mo(PMe_3)$_3$
lattice	orthorhombic	monoclinic
formula	$C_{19}H_{35}MoP_3$	$C_{23}H_{37}BMoP_3$
formula weight	452.32	502.38
space group	*Pbca*	$P2_1$
a/Å	16.0464(19)	9.5584(7)
b/Å	9.5126(12)	16.3202(13)
c/Å	29.522(4)	16.2667(13)
α/°	90	90
β/°	90	94.116(1)
γ/°	90	90
V/Å^3	4506.3(10)	2531.0(3)
Z	8	4
temperature (K)	243	243
radiation (λ, Å)	0.71073	0.71073
ρ(calcd), g cm^{-3}	1.333	1.318
μ(Mo Kα), mm^{-1}	0.794	0.714
θ_{max}, °	25.0	28.2
no. of data	3945	10652
no. of parameters	209	488
R_1	0.0925	0.0267
wR_2	0.1584	0.0631
GOF	1.210	1.033

Computational Details. All calculations were initially carried out using DFT as implemented in the Jaguar 4.0, 4.1, and 6.0 suites of ab initio quantum chemistry programs.[39] Initial geometries were obtained from crystal structures when available, and in other cases the desired molecule was built through modification of the coordinates of a similar compound with known structure. The PH_3 ligand was used instead of PMe_3 for computational expediency. Geometry optimizations were performed with the B3LYP density functional[40] and the 6-31G** basis set for C, H, N, and P, while Mo was represented using the Los Alamos LACVP basis set[41] that includes relativistic effective core potentials. No structure constraint was used during the geometry optimization unless otherwise specified. The energies of the optimized structures were re-evaluated by additional single-point calculations on each optimized geometry using the cc-pVTZ(-f) correlation-consistent triple-ζ basis set for C, H, N, and P, and LACV3P for Mo.

The structures of (η^6-AnH)Mo(PH_3)$_3$ and (η^6-NpH)Mo(PH_3)$_3$ were obtained by replacing PMe_3 ligands in the crystal structures of (η^6-AnH)Mo(PMe_3)$_3$ and (η^6-NpH)Mo(PMe_3)$_3$ with PH_3 ligands, respectively, followed by geometry optimization. The structure of (η^6-PhH)Mo(PH_3)$_3$ was obtained by modifying the structure of (η^6-NpH)Mo(PH_3)$_3$ as a starting point prior to geometry optimization.

The structure of (η^4-AnH)Mo(PMe_3)$_3H_2$ was obtained by adding two hydride ligands to the molybdenum center of (η^6-AnH)Mo(PH_3)$_3$ prior to geometry optimization. The structure of (η^4-AnH)Mo(PH_3)$_3H_2$ so obtained was used as a starting point to evaluate the stability of other conformations that differ by the relative positions of anthracene, PH_3, and hydride ligands. A total of 13 distinct structures of (η^4-AnH)Mo(PH_3)$_3H_2$ were obtained, with the lowest energy structure being 2.0

(36) NMR data are reported in ref 8b.
(37) ^1H NMR data (C_6D_6): 3.63 [s, 4 H of $C_{14}H_{12}$], 7.08 [br, 8 H of $C_{14}H_{12}$]. ^1H NMR data (C_6D_{12}): 3.83 [s, 4 H of $C_{14}H_{12}$], 7.05 [m, 4 H of $C_{14}H_{12}$], 7.14 [m, 4 H of $C_{14}H_{12}$].

(38) Sheldrick, G. M. SHELXTL, *An Integrated System for Solving, Refining and Displaying Crystal Structures from Diffraction Data*; University of Göttingen: Göttingen, Germany, 1981.
(39) Schrödinger, LLC, Portland, OR.
(40) (a) Becke, A. D. *J. Chem. Phys.* **1993**, *98*, 5648−5652. (b) Becke, A. D. *Phys. Rev. A* **1988**, *38*, 3098−3100. (c) Lee, C. T.; Yang, W. T.; Parr, R. G. *Phys. Rev. B* **1988**, *37*, 785−789. (d) Vosko, S. H.; Wilk, L.; Nusair, M. *Can. J. Phys.* **1980**, *58*, 1200−1211. (e) Slater, J. C. *Quantum Theory of Molecules and Solids, Vol. 4: The Self-Consistent Field for Molecules and Solids*; McGraw-Hill: New York, 1974.
(41) (a) Hay, P. J.; Wadt, W. R. *J. Chem. Phys.* **1985**, *82*, 270−283. (b) Wadt, W. R.; Hay, P. J. *J. Chem. Phys.* **1985**, *82*, 284−298. (c) Hay, P. J.; Wadt, W. R. *J. Chem. Phys.* **1985**, *82*, 299−310.

kcal mol^{-1} more stable than the second most stable geometry; the other conformations examined are considerably less stable (7.8−18.1 kcal mol^{-1}) than the lowest energy structure. The computational result that there is a conformer of (η^4-AnH)Mo(PH_3)$_3H_2$ which is only slightly higher in energy than the ground state is consistent with low-temperature ^{1}H and ^{31}P NMR spectroscopic studies (vide infra). The NMR spectroscopic data also indicate that the lowest energy structure possesses C_1 symmetry, whereas the higher energy structure possesses C_s symmetry, in accord with the calculations.

The structures of (η^4-PhH)Mo(PH_3)$_3H_2$ and (η^4-NpH)Mo(PH_3)$_3H_2$ were obtained by modifying each of the 13 geometries of (η^4-AnH)-Mo(PH_3)$_3H_2$ followed by geometry optimization. In both cases, the most stable structures of (η^4-PhH)Mo(PH_3)$_3H_2$ and (η^4-NpH)Mo(PH_3)$_3H_2$ display an overall similarity to that of (η^4-AnH)Mo(PH_3)$_3H_2$.

Molecular orbital analyses were performed with the aid of JIMP,[42] which employs Fenske−Hall calculations[43] and visualization using MOPLOT.[44] Analysis of the back-bonding interactions in (η^6-ArH)-Mo(PH_3)$_3$ and (η^4-ArH)Mo(PH_3)$_3H_2$ was performed by utilizing the fragment partitioning method[45,46] as employed in the Amsterdam Density Functional program suite (ADF 2004.01).[47,48] ADF geometry optimizations were performed with the BP86 functional,[40b,49] and the all-electron, Slater-type orbital (STO) basis sets employed were of triple-ζ quality augmented with two polarization functions and incorporated relativistic effects using the zero-order regular approximation (ADF basis ZORA/TZ2P).[50−52] After full geometry optimization, the Mo−arene complex of interest was partitioned into its constituent fragments, e.g., ArH ($^1A_1$) and Mo(PH_3)$_3$ ($^1A_1$) for (η^6-ArH)Mo(PH_3)$_3$. Single-point calculations were performed using the BLYP functional[40b,c] with a triple-ζ quality basis set augmented with one polarization function that also includes scalar relativistic effects (ADF basis ZORA/TZP).[50−52] For the Mo atoms, the 1s2s2p3s3p3d core of electrons was treated with the frozen-core approximation. To ascertain the binding interactions between the fragments, recombination of the original complex was performed via a single-point calculation using the constituent fragments to describe the final Kohn−Sham orbitals as linear combinations of fragment orbitals. The composition and interaction between Mo and arene fragment orbitals within the individual molecular orbitals of the complex was determined by correlating the individual symmetrized fragment orbital (SFO) energies and overlap populations calculated as part of the standard ADF output.

Conclusions

In conclusion, the increased facility of naphthalene and anthracene to adopt η^4-coordination modes compared to that of benzene is not a consequence of a reduced loss of resonance energy for the arene fragment, but is rather a consequence of the fact that the Mo−(η^4-ArH) bonding interaction increases in the sequence benzene < naphthalene < anthracene, while the Mo−(η^6-ArH) bonding interaction exhibits the opposite trend. As a consequence, oxidative addition of H_2 to (η^6-AnH)-Mo(PMe_3)$_3$ is much more thermodynamically favored than oxidative addition to (η^6-PhH)Mo(PMe_3)$_3$.

Acknowledgment. We thank the U.S. Department of Energy, Office of Basic Energy Sciences (DE-FG02-93ER14339), for support of this research and Professor Daniel G. Nocera for generous access to his computational facility. Professor Mu-Hyun Baik, Professor Todd Marder, and the reviewers are thanked for their helpful comments and advice which significantly improved the quality of this article.

Supporting Information Available: Cartesian coordinates for geometry-optimized structures (PDF); crystallographic data for (η^6-NpH)Mo(PMe_3)$_3$ and (η^6-AnH)Mo(PMe_3)$_3$ (CIF). This material is available free of charge via the Internet at http://pubs.acs.org.

JA058107F

(42) Manson, J.; Webster, C. E.; Hall, M. B. JIMP Development Version 1.1.5, 2005 (built for Windows PC and Redhat Linux 7.3); Department of Chemistry, Texas A&M University, College Station, TX 77842 (http://www.chem.tamu.edu/jimp/).
(43) Hall, M. B.; Fenske, R. F. *Inorg. Chem.* **1972**, *11*, 768−775.
(44) Lichtenberger, D. L. Version 2.0, June 1993; Department of Chemistry, University of Arizona, Tuscon, AZ 85721.
(45) (a) Morokuma, K. *J. Chem. Phys.* **1971**, *55*, 1236−1244. (b) Morokuma, K. *Acc. Chem. Res.* **1977**, *10*, 294−300.
(46) (a) Ziegler, T.; Rauk, A. *Theor. Chim. Acta* **1977**, *46*, 1−10. (b) Ziegler, T.; Rauk, A. *Inorg. Chem.* **1979**, *18*, 1558−1565. (c) Ziegler, T.; Rauk, A. *Inorg. Chem.* **1979**, *18*, 1755−1759.
(47) ADF 2004.01; SCM, Theoretical Chemistry, Vrije Universiteit, Amsterdam, The Netherlands (http://www.scm.com).
(48) te Velde, G.; Bickelhaupt, F. M.; van Gisbergen, S. J. A.; Fonseca Guerra, C.; Baerends, E. J.; Snijders, J. G.; Ziegler, T. *J. Comput. Chem.* **2001**, *22*, 931−967 and references therein.
(49) (a) Perdew, J. P. *Phys. Rev. B* **1986**, *34*, 7406−7406. (b) Perdew, J. P. *Phys. Rev. B* **1986**, *33*, 8822−8824.
(50) van Lenthe, E.; Baerends, E. J.; Snijders, J. G. *J. Chem. Phys.* **1993**, 99, 4597−4610.
(51) van Lenthe, E. The ZORA Equation. Thesis, Vrije Universiteit Amsterdam, The Netherlands, 1996.
(52) Faas, S.; Snijders, J. G.; van Lenthe, J. H.; van Lenthe, E. Baerands, E. J. *Chem. Phys. Lett.* **1995**, *246*, 632−640.